On the computation of acoustic modes of cavities with irregular shapes

J. Missaoui and L. Cheng
Department of Mechanical Engineering
Laval University Quebec, Canada, G1K 7P4

1. Introduction

Reducing noise level needs a better understanding of the mechanism of noise transmission into cavities. For this purpose and due to the large number of degree of freedom needed for the Finite Element Method, more physical methods are needed to calculate the acoustic properties with less time computation, it is especially the case when the sound and structure are coupled. Among them one finds the following ones: Green function method based development [1] and the acoustoelastic theory [2]–[3]. The first one, similar to that used in ref. [4], considers a perturbation in the boundary shape. The second one is based on a subdivision of the interior space to a series of rectangular sub-cavities connected by vibrating membranes. Due to the reasonable deviation of the irregular cavity considered as a limitation in the Green function method and the increased number of sub-cavities used in the acoustoelastic theory, an alternative approach which is a combination of the two cited methods is presented. A major advantage of the proposed method is that analytical expressions for regular sub-cavities can be used while others can be characterized by a linear combination of the known eigenfunction of their bounded cavities.

2. Modelling of the acoustic properties

Based on Green theorem, the acoustic pressure inside a cavity can be expressed as an integral equation including the boundary and the membrane effects .

$$p_c = \int_{S_b} (G\frac{\partial p}{\partial \mathbf{n}} - p\frac{\partial G}{\partial \mathbf{n}})ds + \int_{S_m} (G\frac{\partial \bar{p}}{\partial \mathbf{n}} - \bar{p}\frac{\partial G}{\partial \mathbf{n}})ds \quad (1)$$

where: G is Green's function for a Neumann boundary, $\mathbf{n}$ is the outward normal vector of the boundary surface S_b, $\bar{p}$ is the pressure drop across the membrane S_m, c is the sound speed inside the cavity.

In the combined approach (see Figure 1), the acoustic pressure inside irregular sub-cavity is expressed as a linear combination of a know orthogonal functions: $\psi(r) = \sum_n A_n \phi_n(r)$ ($\phi_n(r)$ represents the spatial shape of the regular sub-cavity enclosing the irregular one). By a physical observation, if the approximated cavity presents a large deviation with respect to the bounding one, a minimal subdivision of the irregular cavity is necessary. A membrane without rigidity and mass is imagined to exist separating the two sub-cavities. Using equation (1), and allowing a continuous pressure across the membrane, the final coupled modal equations are derived as a function of the modal coordinate q_m of the vibrating membrane *in vacuo*.

$$A_n^i(\Lambda_n^{i2} - \omega^2)V_i M_n^i = -\rho c^2 \sum_m \ddot{q}_m L_{nm}^{ii} \quad (2)$$

$$A_n^j(\Lambda_n^{j2} - \omega^2)V_j M_n^j + c^2 \sum_{n'} A_{n'} B_{nn'} = \rho c^2 \sum_m \ddot{q}_m L_{nm}^{ij}$$

$$\bar{p} = 0 : \sum_n b_n^i L_{nm}^{ii} = \sum_n b_n^j L_{nm}^{ij}$$

where L_{nm}^{ij} is the modal acoustoelastic coupling coefficient between membrane (i) and hard walled mode of sub-cavity (j), the term $B_{nn'} = \int_s \phi_{n'} \frac{\partial \phi_n}{\partial \mathbf{n}} ds$ can be done analytically or numerically depending on the irregularity of the sub-cavity shape.
It should be noted that the proposed approach is in fact an extension of the Green function method by taking advantage that certain sub-cavities of regular shape may exist in the whole system.

3. Illustrative example

Figure 2 shows a cross-section of an irregular cylindrical cavity used to predict the acoustic characteristics inside a simplified aircraft cabin. Only natural acoustic frequencies are presented and compared to published results calculated by Finite difference method [5]. In Table 1, the Green function method using the cylindrical bounding cavity modes is used for a floor angle

($\theta_f = 49°$). Better results can be obtained for a reasonable deviation of the irregular cavity from the cylindrical one. In Table 2, results obtained by the combined approach are presented and compared to the Finite difference method.

4. Conclusion

It was shown that it is possible to use a combined analytical approach for the determination of the acoustic characteristics. This approach permits a minimal discretization of the irregular cavity, a saving in computational time compared to the acoustoelastic approach. However, the Green function method seems to be more accurate when the irregular cavity does not present a large deviation in boundary shape when compared to its bounding regular cavity.

References

[1] G. P. Succi 1987 *JASA*. 81(6),1688–1694. The interior acoustic field of an automobile cabin.

[2] E.H. Dowell, G.F. Gorman, and D.A. Smith 1977 *JSV* 52(4),519–542. Acoustoelasticity: General theory, acoustic natural modes and forced response to sinusoidal excitation, including comparison with experiment.

[3] Chao, Chen-Fu B. 1981 *Modal Analysis of interior noise fields* Ph.D. thesis Princeton University

[4] P.M. Morse and H. Feshbach 1953 *Methods of Theoretical Physics*

[5] L.D. Pope, E.G. Wilby and J.F. Wilby 1984 *Analytical predictor of the interior noise for cylindrical models of Aircraft fuselage for prescribed exterior noise fields*

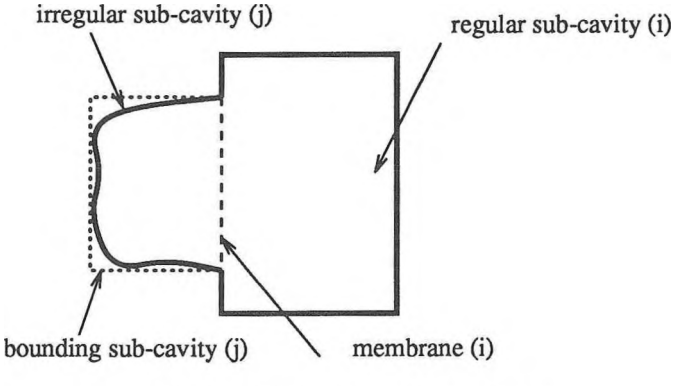

Figure 1: Combined approach

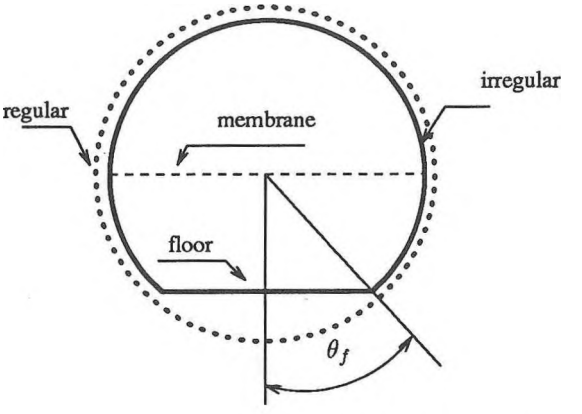

Figure 2: Irregular cylindrical cavity

Table 1: Finite difference and Green function method

Mode	Ref. [5]	Green function method	
	f_n (Hz)	f_n (Hz)	Error (%)
1	96.416	96.210	-0.21
2	113.002	114.847	1.63
3	166.997	169.457	1.45
4	178.748	179.937	0.66
5	212.718	217.642	2.26
6	238.019	243.739	2.31
7	243.915	246.772	1.17
8	280.915	284.653	1.33
9	283.663	286.643	1.05
10	305.542	295.714	-3.21

Table 2: Finite difference and Combined approach

Mode	Ref. [5]	Present work	
	f_n (Hz)	f_n (Hz)	Error (%)
1	96.416	96.5	0.080
2	113.002	116.0	2.65
3	166.997	166.25	-0.44
4	178.748	180.5	0.98
5	212.718	213.25	0.25
6	238.019	230.0	-3.37
7	243.915	246.0	0.85
8	280.915	278.0	-1.03
9	283.663	290.0	2.23
10	305.542	294.75	-3.53